www.nature.com/aps

Acta Pharmacologica Sinica

ARTICLE

S-nitrosylation of c-Jun N-terminal kinase mediates pressure overload-induced cardiac dysfunction and fibrosis

Miao Zhou[1], Ji-yu Chen[1], Meng-Lin Chao[1], Chao Zhang[1], Zhi-guang Shi[2], Xue-chun Zhou[1], Li-ping Xie[1,2], Shi-xiu Sun[1], Zheng-rong Huang[3], Shan-shan Luo[1] and Yong Ji[1,2,4]

Cardiac fibrosis (CF) is an irreversible pathological process that occurs in almost all kinds of cardiovascular diseases. Phosphorylation-dependent activation of c-Jun N-terminal kinase (JNK) induces cardiac fibrosis. However, whether S-nitrosylation of JNK mediates cardiac fibrosis remains an open question. A biotin-switch assay confirmed that S-nitrosylation of JNK (SNO-JNK) increased significantly in the heart tissues of hypertrophic patients, transverse aortic constriction (TAC) mice, spontaneously hypertensive rats (SHRs), and neonatal rat cardiac fibroblasts (NRCFs) stimulated with angiotensin II (Ang II). Site to site substitution of alanine for cysteine in JNK was applied to determine the S-nitrosylated site. S-Nitrosylation occurred at both Cys116 and Cys163 and substitution of alanine for cysteine 116 and cysteine 163 (C116/163A) inhibited Ang II-induced myofibroblast transformation. We further confirmed that the source of S-nitrosylation was inducible nitric oxide synthase (iNOS). 1400 W, an inhibitor of iNOS, abrogated the profibrotic effects of Ang II in NRCFs. Mechanistically, SNO-JNK facilitated the nuclear translocation of JNK, increased the phosphorylation of c-Jun, and induced the transcriptional activity of AP-1 as determined by chromatin immunoprecipitation and EMSA. Finally, WT and iNOS$^{-/-}$ mice were subjected to TAC and iNOS knockout reduced SNO-JNK and alleviated cardiac fibrosis. Our findings demonstrate an alternative mechanism by which iNOS-induced SNO-JNK increases JNK pathway activity and accelerates cardiac fibrosis. Targeting SNO-JNK might be a novel therapeutic strategy against cardiac fibrosis.

Keywords: cardiac fibrosis; S-nitrosylation; transcriptional activation; JNK; iNOS

Acta Pharmacologica Sinica (2022) 43:602–612; https://doi.org/10.1038/s41401-021-00674-9

INTRODUCTION

Cardiac fibrosis is a process of structural and functional changes in the left ventricle (LV) including abnormal proliferation of fibroblasts, expression of pro-fibrotic genes and deposition of extracellular collagen [1, 2]. Cardiac fibrosis is related to most of heart diseases, including cardiac arrhythmias, dilated cardiomyopathy, and congestive heart failure [3].

Transverse aortic constriction (TAC) results in cardiac hypertrophy and fibrosis through peripheral resistance and cardiac afterload, which is similar to the pathology of human hypertension [4–6] In addition, the activation of endocrine factors, especially Ang II, can initiate a large number of signalling pathways through the Ang II type 1 receptor (AT1R), which consequently transits extracellular mechanical stress to intracellular kinase cascades [7, 8]. The mitogen-activated protein kinase (MAPK) pathway is an essential downstream component of AT1R. Abnormal activation of MAPKs exacerbates oxidative stress and inflammation in the cardiovascular system [9–11]. c-Jun N-terminal kinase (JNK), a protein serine/threonine kinase, belongs to the MAPK family [12]. It was originally identified as a protein kinase that specifically phosphorylates the N-terminal transactivation domain of the transcription factor c-Jun at Ser63 and Ser73 [13], which subsequently activates the activator protein-1 (AP-1) [14] to induce the expression of profibrotic genes, such as *Col1a1*, *Col3a1*, and *Acta2*. Interestingly, the antioxidant N-acetylcysteine restrains the activation of JNK to a lesser extent in ischaemia/reperfusion injury, indicating an alternative mechanism of JNK activation [15].

Nitric oxide (NO) was first identified as an endothelium-derived relaxing factor that relaxes vascular smooth muscle, in part by activating guanylate cyclase [16]. The importance of NO-induced vascular relaxation is well-characterized. However, at the same time, the oxidative modification of cysteine by nitric oxide (NO) to form the protein S-nitrosothiol, mediates the multiple roles of NO in cellular functions [17]. Numerous studies have demonstrated that S-nitrosylation is a universal post-translational modification that affects protein function, distribution, and interaction with other proteins [18]. Multiple roles of S-nitrosylation have been found under pathological conditions in endothelial cells [19], cardiomyocytes [20], macrophages [21], microglia [22], and neurons [23]. A previous study has revealed that JNK activation was negatively controlled by S-nitrosylation at Cys116 in murine macrophage cells [24]. However, questions such as whether the S-nitrosylation of JNK (SNO-JNK) is involved in the development of TAC-induced myocardial fibrosis, which cysteine residue(s) is(are)

[1]Key Laboratory of Cardiovascular and Cerebrovascular Medicine, Nanjing Medical University, Nanjing 201203, China; [2]Key Laboratory of Targeted Intervention of Cardiovascular Disease, Collaborative Innovation Center for Cardiovascular Disease Translational Medicine, Nanjing Medical University, Nanjing 201203, China; [3]Department of Cardiology, the First Affiliated Hospital of Xiamen University, Xiamen 361003, China and [4]State Key Laboratory of Reproductive Medicine, Nanjing Medical University, Nanjing 201203, China
Correspondence: Zheng-rong Huang (huangzhengrong@xmu.edu.cn) or Shan-shan Luo (njmulss@njmu.edu.cn) or Yong Ji (yongji@njmu.edu.cn)
These authors contributed equally: Miao Zhou, Ji-yu Chen

Received: 3 January 2021 Accepted: 31 March 2021
Published online: 19 May 2021

modified and how this modification affects JNK activity and the progression of cardiac fibrosis remain unknown.

Here, we clarify the roles of SNO-JNK in the progression of cardiac fibrosis. The level of SNO-JNK was obviously increased in different models of cardiac fibrosis, and S-nitrosylation of JNK at both Cys116 and Cys163 accelerated cardiac fibrosis by activating c-Jun phosphorylation and transcriptional activation of AP-1. iNOS was the endogenous source of S-nitrosylation of JNK, as SNO-JNK was reduced in $iNOS^{-/-}$ mice subjected to TAC, compared with that in WT mice. These results illustrate an alternative activation of the JNK pathway and imply a candidate crosstalk between iNOS and the MAPK signalling pathway in the process of cardiac fibrosis.

MATERIALS AND METHODS

Human heart samples

Human heart tissue samples were collected during the cardiac valve replacement surgery, the samples were classified into non-myocardial hypertrophic group and myocardial hypertrophic group according to echocardiographic findings prior to the surgery. The study confirmed to the principles outlined in the Declaration of Helsinki. Written informed consent was obtained from all patients. The study protocol was approved by the Ethics Committee of the First Affiliated Hospital of Xiamen University (approval no. KYZ-2014-007). Clinical characteristics of the patients recruited are shown in Supplementary Table S1.

Animals

Adult C57BL/6 mice and spontaneously hypertensive rats (SHRs) were provided by the Experimental Animal Center of Nanjing Medical University. $iNOS^{-/-}$ mice were kind gifts of Dana-Farber Cancer Institute, Harvard Medical School (USA). All animals were kept under standard animal room conditions (temperature 21 ± 1 °C; humidity 55%–60%; 12 h light: dark cycles) and had free access to food and water. All animal experiments were approved by the Committee on Animal Care of Nanjing Medical University and were conducted according to the NIH Guidelines for the Care and Use of Laboratory Animals. All studies involved with animals were reported in accordance with the ARRIVE guidelines.

Transverse aortic constriction (TAC) surgery

Eight-week-old male C57BL/6 or $iNOS^{-/-}$ mice were anesthetized with 3.5% isoflurane and maintained with 2.0% isoflurane during the surgery, and secured to an operating table with an electric heating device. A midline cervical incision was made to expose the trachea. The cannula was connected to a volume cycled rodent ventilator after successful endotracheal intubation. The chest was opened and the thoracic aorta was identified. A 7-0 silk suture was placed around the transverse aorta and tied around a 26-gauge blunt needle, which was subsequently removed. After 4 weeks, the survival mice were sacrificed and the hearts were quickly excised.

Echocardiography

Cardiac functions were assessed by the echocardiography with a 30-MHz small animal color ultrasonic diagnostic apparatus (Visual Sonic Vevo 2100). The LV mass, interventricular septum (IVS), left ventricular posterior wall (LVPW), ejection fraction (EF), and fractional shortening (FS) were calculated with VEVO Analysis software (version 2.2.3).

Isolation of neonatal rat cardiac fibroblasts and cell culture

1–3-day-old Sprague Dawley rats were provided by the Experimental Animal Center of Nanjing Medical University. Enzymatic digestion was used to extract neonatal rat cardiac fibroblasts (NRCFs). Briefly, Neonatal Sprague Dawley rats were sacrificed and hearts were removed immediately in a sterilized environment. The residual blood clots and atria were removed in DMEM and the hearts were cutted into pieces. The heart tissues were digested by incubated with 0.25% Trypsin-EDTA in water bath at 37 °C for 5 min. The supernatant was collected and neutralized with 20% FBS. The above processes were repeated for 7–10 times until the tissues were digested completely. The collected cell suspension was centrifuged at 2000 rpm for 10 min. The precipitates were resuspended in DMEM with 10% FBS. Cells were plated in a 10 cm cell culture plate and cultured at 37 °C in a humidified incubator with 5% CO_2. After 3 h, the medium was replaced with fresh DMEM (7–10 mL) containing 10% FBS. Thirty-six hours after plating, the neonatal myocardial fibroblasts were stimulated by angiotensin II (Ang II; 100 nM, Sigma-Aldrich, St Louis, USA) or 1400 W (10 μM; Sigma-Aldrich, St Louis, USA) for further experiments. Human embryonic kidney 293 (HEK293) cells were purchased from the American Type Culture Collection (Rockville, MD, USA) and cultured in DMEM with 10% (v/v) FBS.

Plasmids transfection

Plasmids containing FLAG-JNK-WT, FKAG-JNK-C116A, FKAG-JNK-C163A, and FLAG-JNK-116/163A were constructed from SinoBio (Beijing, China). Plasmids were transfected into 75% confluent HEK293 cells or NRCFs with Lipofectamine 3000 reagent (Invitrogen). After 4–6 h of transfection, medium was changed to fresh DMEM, and cells were maintained for an additional 24 h before used.

Biotin switch assay for detection of S-nitrosylation

S-nitrosylated proteins were detected using biotin switch assay as reported previously [25–27]. In brief, cells were incubated with blocking buffer containing 50 mM N-ethylmaleimide at 50 °C for 30 min to block free cysteines. Proteins were precipitated with cold acetone, washed and resuspended in 10 mM of ascorbic acid (Vc) buffer containing biotin-maleimide at room temperature for 2 h to reduce NO group into thiols residues, and to label the free thiols with biotin. The samples without ascorbic acid incubation were used as negative controls (-Vc). All steps were carried out in the dark. The biotinylated proteins were then purified by NeutrAvidin Plus UltraLink Resin (Thermo Scientific), separated by SDS-PAGE and detected by immunoblotting with JNK antibody.

Western blotting

Western blotting analysis was performed as previously described. Cells were lysed on ice with RIPA lysis buffer supplemented with a protease and phosphatase inhibitor cocktail. After centrifugation, the supernatant was collected and protein concentration was determined using the Bradford Assay. Equal amounts of protein were resolved in 8% or 10% SDS-PAGE and transferred to PVDF membranes (Millipore). Targeting proteins were incubated with the appropriate primary antibodies overnight at 4 °C and the corresponding secondary antibodies for 2 h at room temperature followed by chemiluminescent detection (Bio-Rad). Primary antibodies including anti-JNK antibody (CST, MA, USA), anti-eNOS antibody (CST, MA, USA), anti-nNOS antibody (CST, MA, USA), anti-iNOS antibody (Abcam, Cambridge, UK), anti-c-Jun antibody (CST, MA, USA), anti-p-c-Jun antibody (CST, MA, USA), anti-Collagen I antibody (RockLand, PA, USA), anti-α-SMA antibody (Abcam, Cambridge, UK), anti-GSNOR antibody (Abcam, Cambridge, UK), anti-Trx antibody (Abcam, Cambridge, UK), and anti-GAPDH antibody (Bioworld, Wuhan, China). The band intensities were analyzed by Image-Pro Plus 8.0 software.

Immunofluorescence staining

Cells were washed with PBS and fixed with 4% paraformaldehyde, permeabilized with 0.03% Triton X-100 and blocked with 3% BSA. The cells were immunized with anti-α-SMA antibodies overnight at 4 °C, followed by incubated with secondary antibodies conjugated with Alexa-594 (Life Technologies, Carlsbad, USA) for 1 h at room temperature. Cell nucleus were counterstained by DAPI (Yeasen,

Shanghai, China). Confocal microscope (Zeiss LSM 410, Oberkochen, Germany) was used for imaging.

Quantitative real-time PCR analysis

Total RNA was extracted using RNAiso Plus (Takara, Japan) and cDNA was synthesized using HiScript II Q RT SuperMix for qPCR Kit (Vazyme, China). Quantitative PCR was performed by ChamQ™ SYBR® qPCR Master Mix (Vazyme, China). The primer sequences used were shown in Supplementary Table 2.

EMSA

Nuclear protein was extracted using nuclear and cytoplasmic extraction reagents. Double-stranded oligonucleotides containing the AP-1 recognition sequences (5′-CGC TTG ATG ACT CAG CCG GAA-3′) were 3′ end-labelled with biotin. Electrophoretic Mobility Shift Assay (EMSA) was performed to detect the binding activity of AP-1. Specificity of the DNA-protein complex was confirmed by competition with a 100-fold molar excess of unlabeled double-stranded oligonucleotides added to the mixture.

ChIP analysis

Chromatin immunoprecipitation (ChIP) was performed according to the reported method [28] with minor modifications. Briefly, NRCFs were cross-linked with formaldehyde (to a final concentration of 1%) for 10 min at 37 °C. The cross-linking was stopped by adding glycine to a final concentration of 0.125 M. Cells were washed twice with ice-cold PBS and incubated with 500 μL lysis buffer (150 mM NaCl, 25 mM Tris-HCl pH 7.5, 1% Triton X-100, 0.1% SDS, 0.5% deoxycholate) supplemented with protease inhibitor and PMSF. Next, the DNA in cells were sonicated into 200–700 bp fragments using the Sonics Vibra VCX150. The fragmented chromatin was centrifuged at 13,000 ×*g* for 15 min and the supernatants were collected. 50 μL of lysate was referred as input. Protein A/G Sepharose beads were incubated with blocking solution (100 μg of salmon sperm DNA/mL, 500 μg of BSA/mL) at 4 °C for 1 h. Aliquots of lysates containing 200 μg of protein were used for each immunoprecipitation reaction with anti-AP-1 antibody (CST, MA, USA) or pre-immune IgG (CST, MA, USA) at 4 °C, with overnight rocking. On the following day, the beads were washed twice with Low Salt buffer (150 mM NaCl, 20 mM Tris-HCl, 0.1% SDS, 0.5% sodium deoxycholate, 1 mM EDTA, 1% NP-40), twice with High Salt buffer (500 mM NaCl, 20 mM Tris-HCl, 0.1% SDS, 0.5% sodium deoxycholate, 1 mM EDTA, 1% NP-40), twice with LiCl buffer (250 mM LiCl, 20 mM Tris-HCl, 0.1% SDS, 0.5% sodium deoxycholate, 1 mM EDTA, 1% NP-40) and twice with TE buffer (10 mM Tris-HCl, 1 mM EDTA). Immune complexes or input were eluted with the elution buffer (1% SDS, 0.1 M $NaHCO_3$). Cross-linking was reversed by the addition of NaCl (to a final concentration of 0.2 M) at 65 °C overnight. DNA was precipitated by 0.1 volume of 3 M sodium acetate, 1 μL glycogen and 2 volumes of ethanol at −80 °C overnight. Finally, genomic DNA was dissolved in ddH_2O and amplified by real-time PCR. The sequence of primers used were shown in Supplementary Table 3.

Statistical analysis

Data and statistical analyses comply with the recommendations on experimental design and analysis in pharmacology. All data are presented as mean ± standard error of the mean (SEM) of at least three independent experiments ("*n*") if not specifically indicated. Distribution of the data was first analyzed using the Shapiro–Wilk test for analysis of normality. Unpaired two-tailed Student's *t* test was used for comparisons between two groups when data passed normality and equal variance test, otherwise Mann–Whitney *U* test was used. Differences among groups were evaluated using one-way ANOVA followed by Turkey's post-hoc test. Differences were considered statistically significant when $P < 0.05$. All statistical analysis was done with GraphPad Prism version 8.01 (GraphPad Software Inc, San Diego, CA, USA).

RESULTS

S-nitrosylation of JNK increases in hypertrophic murine and human hearts

We first detected S-nitrosylation of JNK (SNO-JNK) in the heart tissues of TAC mice and SHR rats using the well-accepted biotin-switch assay. The levels of SNO-JNK were significantly increased in the heart tissues of SHR rats and TAC mice compared with that in WKY rats and sham-operated mice (Fig. 1a, b). To confirm the clinical relevance of SNO-JNK in the context of cardiac hypertrophy and fibrosis, the levels of SNO-JNK were determined in human myocardium samples collected from non-hypertrophic donors or hypertrophic patients. As expected, SNO-JNK was obviously increased in heart tissues of hypertrophic patients rather than in those of non-hypertrophic donors (Fig. 1c). The protein level of α-SMA was further found to increase significantly in the heart tissues of SHR rats and TAC mice (Fig. 1d, e). Besides, fibrotic-related genes including *Acta2*, *Col1a1*, and *Col3a1* were also increased in heart tissues of TAC mice compared with those in sham-operated mice (Fig. 1f). These results demonstrate that SNO-JNK is associated with cardiac fibrosis.

S-nitrosylation of JNK at cysteine 116/163 induces cardiac fibrosis

S-nitrosylation generally occurs at one or more cysteine sites. To determine which site(s) is (are) responsible for the S-nitrosylation of JNK, we first obtained the full-length sequence of JNK from NCBI and predicted the possible S-nitrosylated sites by a free-available online tool (GPS-SNO, version 1.0). Two cysteine residues, Cys116 and Cys163 were predicted to be available for nitrosylation (Supplementary Fig 1). Based on the predicted result, we constructed JNK expression vectors with mutation from cysteine to alanine at each predicted site (C116A and C163A) and transfected the mutations into HEK293 cells (Supplementary Fig. 2a). Sodium nitroprusside (SNP, 100 μM) was used as an exogenous NO donor to stimulate the S-nitrosylation. The mutations of Cys116 and Cys163 could obviously suppress the increase of SNO-JNK upon SNP, indicating that both Cys116 and Cys163 were involved in the S-nitrosylation of JNK (Fig. 2a). To determine whether S-nitrosylation of Cys116 and Cys163 mediated myofibroblasts differentiation, we further transfected wild-type (WT) JNK, C116A, or C163A mutations into neonatal rat cardiac fibroblasts (NRCFs). Cells were stimulated with Ang II (100 nM) and the levels of Collagen I and α-SMA were determined. Ang II increased the levels of Collagen I and α-SMA in NRCFs overexpressing WT JNK, while either transfection of C116A or C163A reduced the elevation of Collagen I and α-SMA in NRCFs stimulated with Ang II (Supplementary Fig. 2b), indicating that the S-nitrosylation of both Cys116 and Cys163 are involved in myofibroblasts differentiation. To this end, we constructed C116/163A mutation and overexpression of C116/1633A rather than WT JNK alleviated Ang II-induced increase in SNO-JNK (Fig. 2b). Besides, the increases in Collagen I and α-SMA induced by Ang II were inhibited by overexpression of C116/163A rather than WT JNK (Fig. 2c). Furthermore, the mRNA levels of pro-fibrotic markers, including *Acta2*, *Col1a1*, and *Col3a1*, were reduced significantly in NRCFs overexpressing C116/163A compared with WT JNK upon Ang II (Fig. 2d). Finally, the α-SMA level was detected by immunofluorescent staining and C116/163A reduced the immunofluorescent signal of α-SMA in NRCFs stimulated with Ang II as compared with WT JNK (Fig. 2e). EdU incorporation and CCK-8 assay were used to evaluate the proliferation ability of the cardiac fibroblasts, Scratch test and transwell assay were used to detect the migration of fibroblasts. We found that both the proliferation and the migration abilities were increased upon Ang II stimulation in NRCFs overexpressing WT JNK rather than C116/163A mutation (Supplementary Fig. 3). These results demonstrate that the S-nitrosylation of JNK at Cys116/163 induces myofibroblasts differentiation, and inhibition of the S-nitrosylation on Cys116/163 can alleviate cardiac fibrosis.

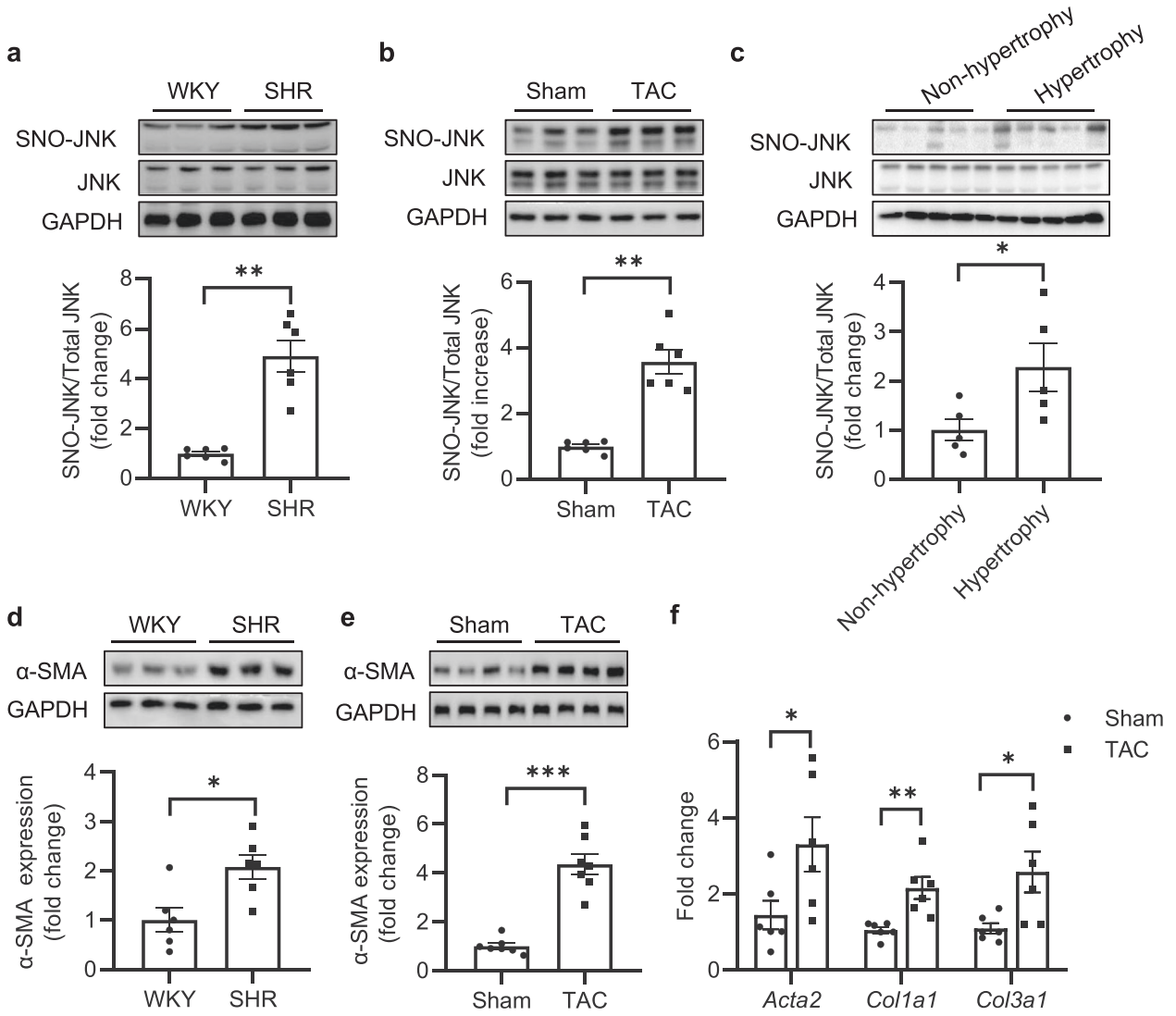

Fig. 1 S-nitrosylation of JNK is increased in hypertrophic murine and human hearts. Nitrosylated proteins were labeled with biotin, purified with streptavidin-sepharose beads and probed for the presence of SNO-JNK in the heart tissues of (**a**) WKY and SHR rats ($n = 6$) (**b**) Sham and TAC mice ($n = 6$), and (**c**) Non-hypertrophy and hypertrophic patients ($n = 5$). The heart tissues of (**d**) WKY and SHR rats ($n = 6$), as well as (**e**) Sham and TAC mice ($n = 7$) were collected and total proteins were extracted, the level of α-SMA expression was determined. **f** Total mRNA was collected from heart tissues of Sham and TAC mice, the levels of *Col1a1* and *Col3a1* and *Acta2* were determined by Q-PCR. $n = 6$. The results are represented as the mean ± SEM. (*$P < 0.05$, **$P < 0.01$, and ***$P < 0.001$). **c**, **d** and mRNA levels of *Acta2*. unpaired *t* test was used for statistical analysis; **a**, **b**, **e** and mRNA levels of *Col1a1* and *Col3a1*. Mann–Whitney test was used for statistical analysis.

S-nitrosylation of JNK induces myofibroblasts differentiation through activating c-Jun/AP-1 pathway

In order to investigate mechanisms underlying myofibroblasts differentiation induced by SNO-JNK, we detected the nuclear translocation of JNK and activity of c-Jun/AP-1 pathway, the main downstream effector of JNK. NRCFs were transfected with WT or C116/163A mutation followed by stimulation with Ang II. As expected, the nuclear translocation of JNK enhanced upon Ang II stimulation in NRCFs overexpressing WT JNK, and overexpression of C116/163A obviously inhibited the increase of nuclear translocation of JNK (Fig. 3a). We then determined the phosphorylation of c-jun (phospho-c-jun) and found an obvious increase of phospho-c-jun in NRCFs expressing WT JNK upon Ang II, which was reduced in cells overexpressing C116/163A (Fig. 3b).

Furthermore, ChIP assay demonstrated that Ang II treatment increased the binding affinity of AP-1 to the promoter of *Acta2*, *Col1a1*, and *Col3a1* in NRCFs overexpressing WT JNK, which was alleviated by the transfection of C116/163A mutation (Fig. 3c). These experiments indicate that S-nitrosylation of JNK at cysteine 116/163 mediates cardiac fibrosis through activating c-Jun/AP-1 pathway.

Inducible nitric oxide synthase (iNOS) is the source of S-nitrosylation of JNK

Nitric oxide (NO) produced by the neuronal (nNOS/NOS1), inducible (iNOS/NOS2) and endothelial (eNOS/NOS3) nitric oxide synthase regulates physiological or pathological processes of cardiac diseases. In contrast, reversible denitrosylation of proteins is mediated by S-nitrosoglutathione reductase (GSNOR) and the thioredoxin (Trx) system. The levels of these enzymes were measured in the hearts of TAC mice, SHR rats, and NRCFs. Increase in iNOS level rather than eNOS or nNOS levels was observed in mice subjected with 4 weeks of TAC (Fig. 4a). Similarly, the increased level of iNOS was observed in heart tissues from the SHR rats rather than from the WKY rats (Fig. 4b). We also observed significant reduction in GSNOR in TAC mice and SHR rats (Fig. 4a, b). However, in NRCFs, increase of iNOS rather than decrease of

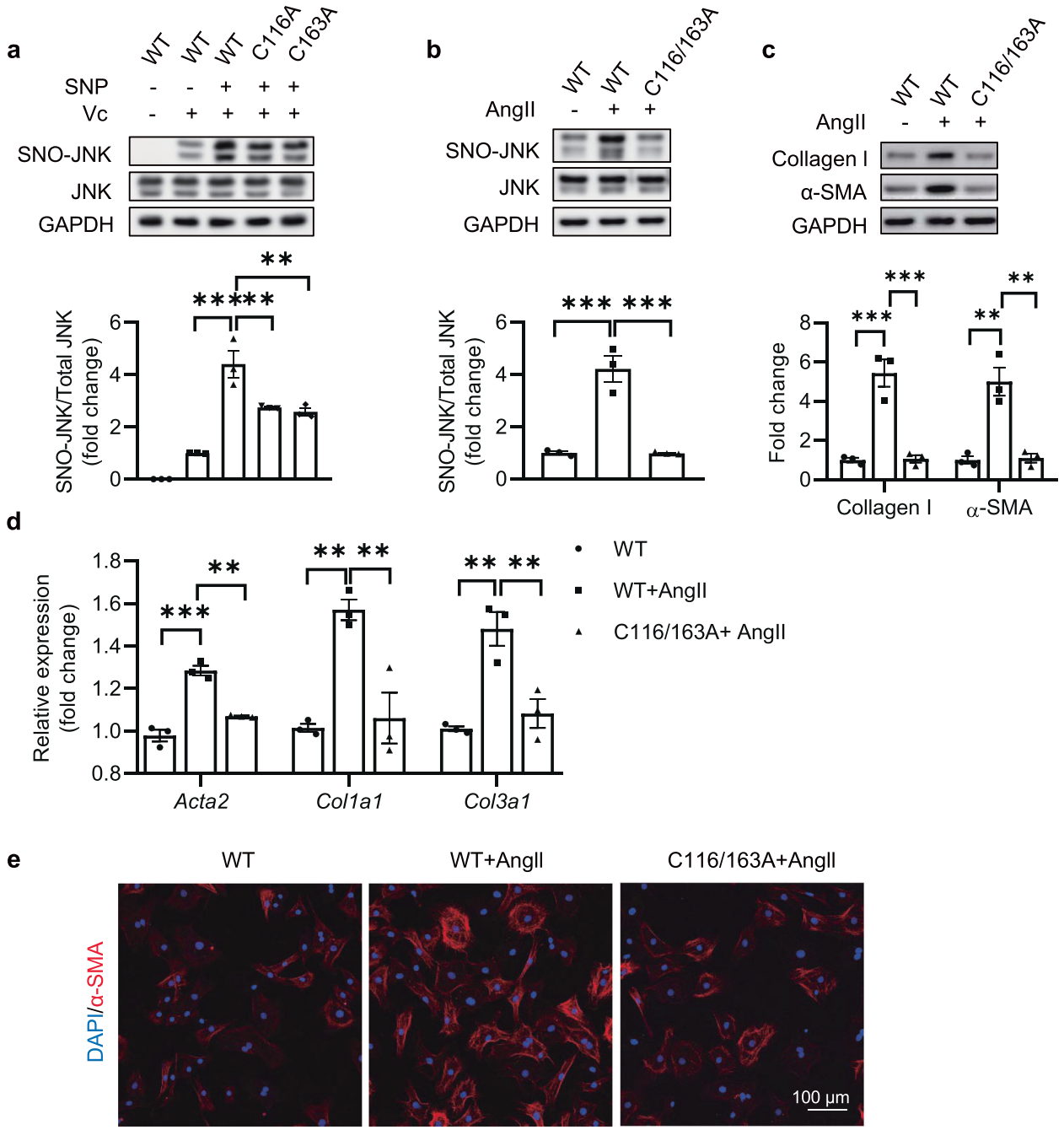

Fig. 2 S-nitrosylation of JNK at cysteine 116/163 promotes cardiac fibrosis. a Wild-type (WT) or site mutated plasmids (C116A and C163A) of JNK were expressed in HEK293 cells, the SNO-JNK in each group was determined by biotin-switch method after treatment with sodium nitroprusside (SNP) (100 μM), lane without ascorbic acid (Vc) as a negative control. $n = 3$ for each group. **b** NRCFs were transfected with WT and C116/163A mutated plasmids, respectively, and stimulated with Ang II (100 nM), the SNO-JNK in each group was determined by biotin-switch method. $n = 3$ for each group. **c** Total protein was extracted and analyzed by SDS-PAGE to determine the levels of collagen I and α-SMA. $n = 3$ for each group. **d** Total mRNA was extracted to determine the levels of *Acta2*, *Col1a1*, and *Col3a1* by Q-PCR. $n = 3$ for each group. **e** Immunofluorescent staining was conducted to determine the in situ expression of α-SMA (Red) and nuclei were counterstained with DAPI (Blue), (Scale Bars: 100 μm). The results are represented as the mean ± SEM. (**$P < 0.01$ and ***$P < 0.001$). One-way ANOVA was used for statistical analysis.

GSNOR was observed upon Ang II (100 nM) treatment (Fig. 4c). We proposed that GSNOR mainly affected the level of protein S-nitrosylation in cardiomyocytes rather than myofibroblasts, as evidenced by our previously published work [27].

To confirm whether elevation of iNOS was responsible for the increased S-nitrosylation of proteins in the presence of Ang II, we detected S-nitrosylation in NRCFs pretreated with iNOS inhibitor 1400 W. The level of S-nitrosylated proteins was increased upon Ang II, which was inhibited by 1400 W (Supplementary Fig 4). As expected, the elevation of SNO-JNK induced by Ang II was accordingly reversed by pretreatment with 1400 W (Fig. 4d). Besides, mRNA levels of *Acta2*, *Col1a1* and *Col3a1* and protein levels of collagen I and α-SMA were partially reduced with 1400 W pretreatment (Fig. 4e, f). Similarly, Immunofluorescent staining demonstrated a reduction in α-SMA staining with 1400 W pretreatment (Fig. 4g). The proliferation and migration of

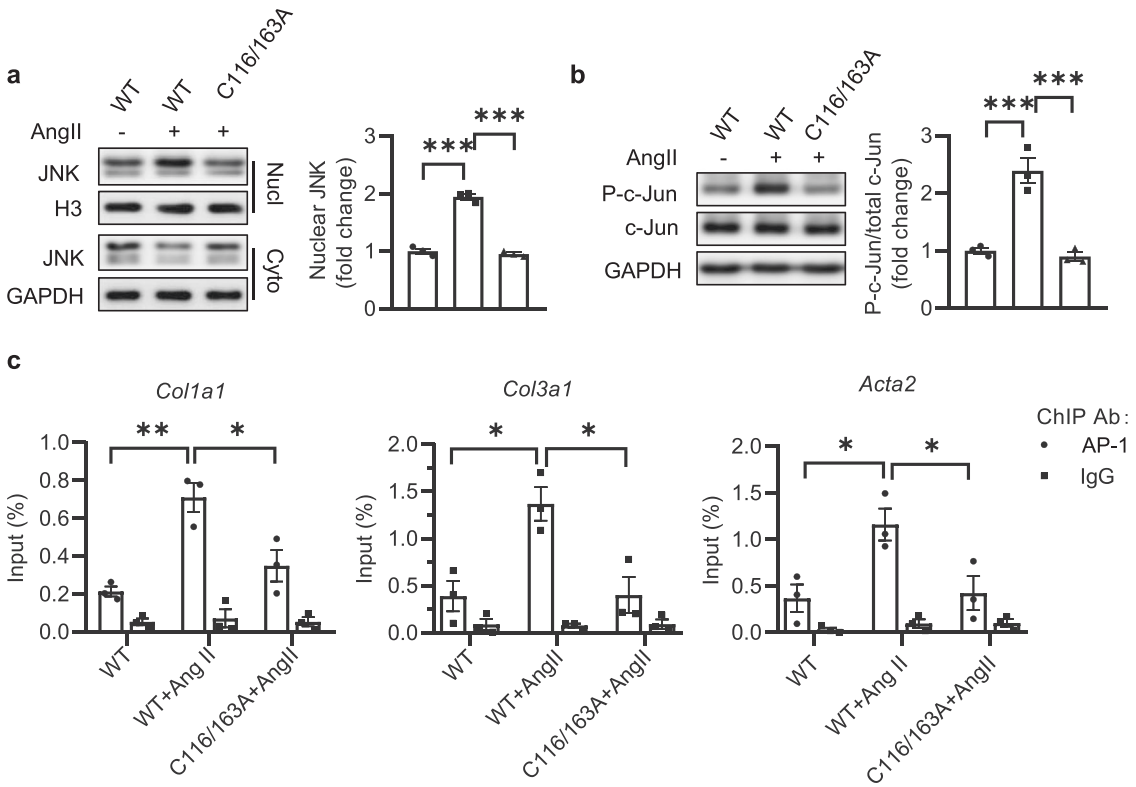

Fig. 3 S-nitrosylation of JNK at cysteine 116 and 163 mediates cardiac fibrosis through activating c-Jun/AP-1 pathway. NRCFs were transfected with WT and C116/163A mutated plasmids, respectively, and stimulated with Ang II (100 nM). **a** Cytoplasmic and nuclear protein was separately extracted and analyzed by SDS-PAGE to determine the level of nuclear JNK. $n = 3$ for each group. **b** Total protein was extracted and analyzed by SDS-PAGE to determine the phosphorylation of c-Jun (P-c-Jun). **c** NRCFs were transfected with WT and C116/163A mutated plasmids, respectively, and stimulated with Ang II (100 nM). ChIP assay was performed to determine the recruitment of AP-1 to the *Col1a1*, *Col3a1*, and *Acta2* promoters with AP-1 antibody. Q-PCR was performed with primers specific for the promoters of *Col1a1*, *Col3a1*, and *Acta2*. IgG was used as an internal negative control. $n = 3$ for each group. The results are represented as the mean ± SEM. (*$P < 0.05$, **$P < 0.01$, and ***$P < 0.001$). One-way ANOVA was used for statistical analysis.

fibroblasts were also inhibited by 1400 W pretreatment as expected (Supplementary Fig. 5).

In order to further investigate whether iNOS-derived NO promoted cardiac fibrosis through increasing SNO-JNK, NRCFs were overexpressed with iNOS and co-transfected with JNK-WT or JNK-C116A/C163A plasmids. As expected, site mutation could reverse the elevation of SNO-JNK (Supplementary Fig. 6a), reduced the upregulation of profibrotic genes including *Acta2*, *Col1a1*, and *Col3a1* (Supplementary Fig. 6b) and inhibited the increase of collagen I and α-SMA (Supplementary Fig. 6c) induced by overexpression of iNOS. Moreover, the enhanced proliferation and migration in NRCFs overexpressing iNOS were reversed by transfection of C116/163A rather than WT JNK (Supplementary Fig. 7). Collectively, these observations indicate that iNOS is the key enzyme mediating SNO-JNK in the context of myofibroblasts differentiation. Inhibition of iNOS is sufficient to alleviate Ang II-induced myofibroblasts differentiation.

iNOS deficiency protects cardiac fibrosis through reducing SNO-JNK

To further discriminate the role of iNOS during cardiac fibrosis in vivo, iNOS$^{-/-}$ mice and WT littermates were subjected to TAC for 4 weeks. Echocardiographic parameters were assessed by a 30-MHz small animal color ultrasonic diagnostic apparatus. Cardiac function was determined by ejection fraction (EF) and fraction shortening (FS). Both EF and FS were significantly reduced in WT mice subjected to TAC (WT TAC), which were recovered in iNOS$^{-/-}$ mice (Fig. 5a, Supplementary Fig. 8b). Besides, iNOS$^{-/-}$ effectively inhibited TAC-induced hypertrophy, as measured by reduced heart size, decreased interventricular septal thickness (IVS), reduced left ventricular posterior wall thickness (LVPW) and HW/BW (Fig. 5a, Supplementary Fig. 8a). The summarization of echocardiographic indexes accordingly indicated the elevation of cardiac functions (Supplementary Table 4).

Masson trichrome and sirius red staining were performed to analyze the collagen deposition. The extent of fibrosis in the interstitial was significantly increased in the WT mice subjected to 4 weeks of TAC compared with that in iNOS$^{-/-}$ TAC mice (Fig. 5b). The level of SNO-JNK was increased robustly in WT mice subjected to TAC rather than in the heart tissues of iNOS$^{-/-}$ mice subjected to TAC (Fig. 5c). The protein level of α-SMA decreased in hearts of iNOS$^{-/-}$ mice compared with that in WT mice subjected to TAC (Fig. 5d). Besides, mRNA levels of *ANP*, *BNP*, *β-MHC* were reduced significanly in hearts of iNOS$^{-/-}$ TAC mice compared with those in WT TAC mice (Fig. 5e). Accordingly, elevation of profibrotic markers including *Acta2*, *Col1a1*, and *Col3a1* was partially reduced in the hearts of iNOS$^{-/-}$ mice after 4 weeks of TAC, compared with those in the hearts of WT TAC mice (Fig. 5f). These results indicate that iNOS deficiency protects TAC-induced cardiac fibrosis through reducing SNO-JNK.

Inhibition of iNOS reduces JNK/c-Jun/AP-1 pathway activity

Next, we determined whether inhibition of iNOS could reduce the aberrant activation of c-Jun/AP-1 pathway. The nuclear translocation of JNK and phosphorylation of c-Jun were determined in the presence of 1400 W upon Ang II (100 nM). As expected, both nuclear translocation of JNK and phosphorylation of c-Jun were significantly reduced in NRCFs pretreated with 1400 W (Fig. 6a, b).

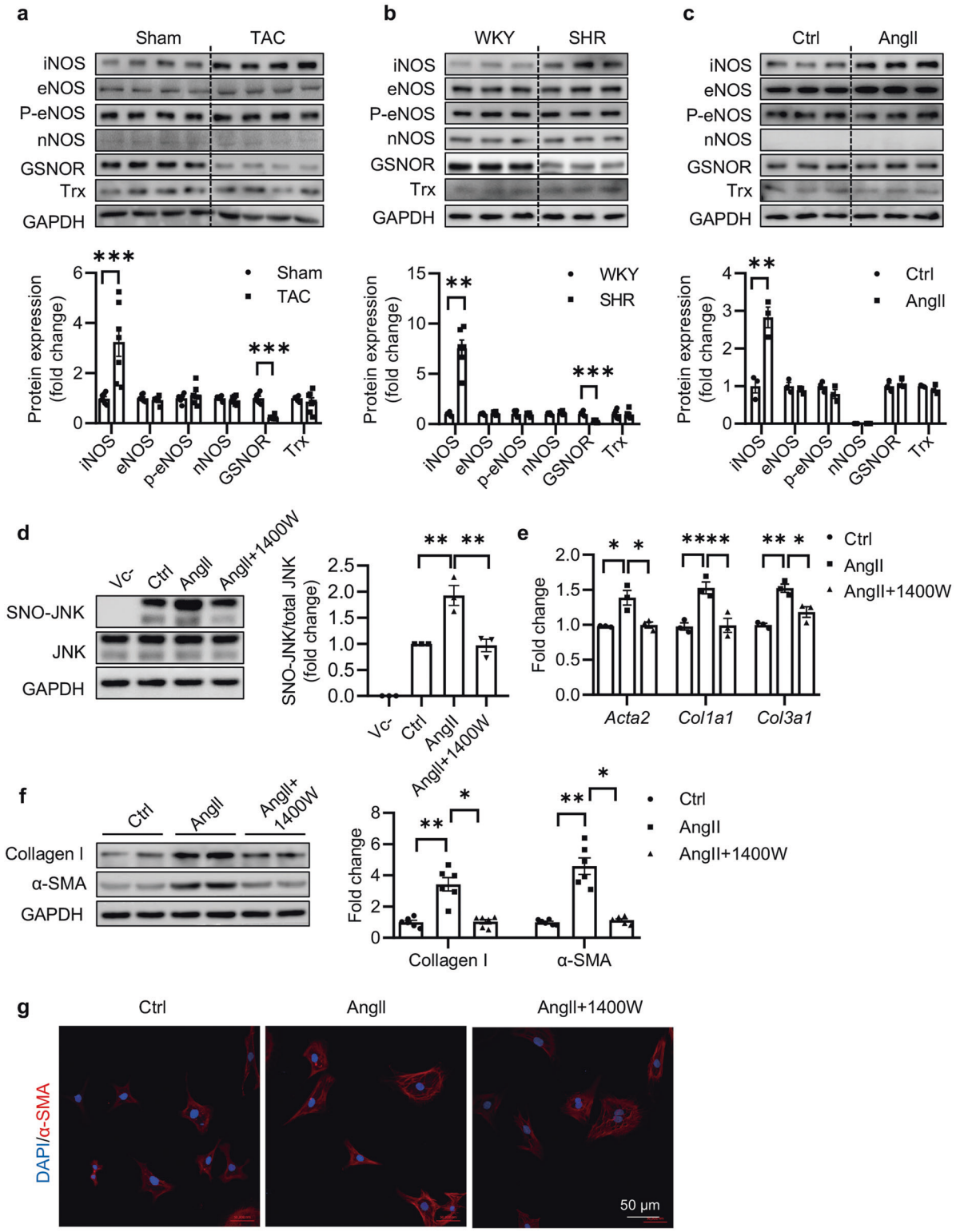

Fig. 4 iNOS promotes Ang II-induced cardiac fibrosis through upregulating SNO-JNK. Protein was extracted and analyzed by SDS-PAGE to determine the levels of iNOS, eNOS, P-eNOS, nNOS, GSNOR and Trx in the heart tissues of (**a**) Sham and TAC mice ($n = 7$) and (**b**) WKY and SHR rats ($n = 6$). **c** NRCFs were treated with Ang II (100 nM), and the protein was extracted and analyzed by SDS-PAGE to determine the levels of iNOS, eNOS, P-eNOS, nNOS, GSNOR, and Trx. $n = 3$ for each group. **d** NRCFs were pre-incubated with 1400 W for 1 h followed by treatment with Ang II (100 nM). Nitrosylated proteins were labeled with biotin, purified with streptavidin-sepharose beads and probed by JNK antibody to determine the level of SNO-JNK. $n = 3$ for each group. **e** Total mRNA was extracted to determine the levels of *Acta2*, *Col1a1*, and *Col3a1* by Q-PCR. $n = 3$ for each group. **f** Total protein was extracted and analyzed by SDS-PAGE to determine the expressions of collagen I and α-SMA. $n = 6$ for each group. **g** Immunofluorescent staining was conducted to determine the in situ expression of α-SMA (Red) and nuclei were counterstained with DAPI (Blue) (Scale Bars: 50 μm). The results are represented as mean ± SEM. (*$P < 0.05$, **$P < 0.01$, and ***$P < 0.001$). **a**, **b**, **c**. Unpaired *t* test was used for statistical analysis; **d**, **e**, **f**. One-way ANOVA was used for statistical analysis.

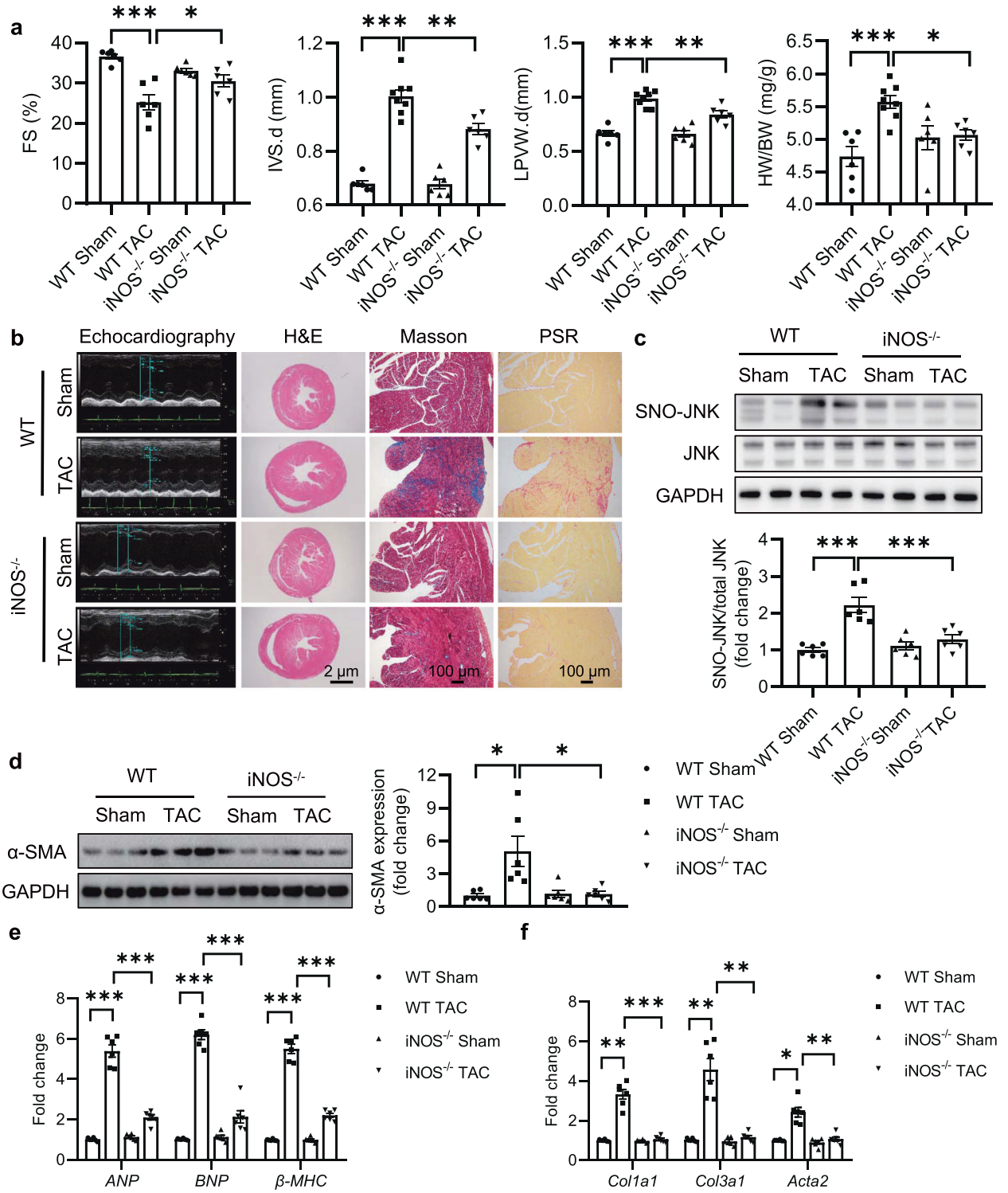

Fig. 5 iNOS knockout protects mice from TAC-induced cardiac fibrosis through reducing SNO-JNK. Eight-week-old C57BL/6 and iNOS-knockout mice were performed with TAC for 4 weeks. **a** Fractional shortening (FS) ($n = 6$), interventricular septum (IVS) ($n = 6$–8), left ventricular posterior wall (LVPW) ($n = 6$–8) and heart weight/Body weight ratios (HW/BW) ($n = 6$–8) were determined. **b** Representative echocardiographic, Hematoxylin & Eosin (HE) staining (Scale Bars: 2 μm), Masson trichrome and picrosirius red staining (Scale Bars: 100 μm) graphs of cardiac section. **c** Heart tissues in each group were collected, nitrosylated protein was labeled with biotin, purified with streptavidin-sepharose beads and probed with JNK antibody to determine the level of SNO-JNK. $n = 6$ for each group. **d** Total protein was extracted and analyzed by SDS-PAGE to determine the level of α-SMA. $n = 6$ for each group. **e**, **f** Total mRNA was collected to determine the levels of *ANP*, *BNP*, *β-MHC*, *Acta2*, *Col1a1*, and *Col3a1* by RT-PCR. $n = 6$ for each group. The results are represented as the mean ± SEM. (*$P < 0.05$, **$P < 0.01$, and ***$P < 0.001$). **a**, **b**, **c**, **e**, and **f** One-way ANOVA was used for statistical analysis; **d** Kruskal–Wallis test was used for statistical analysis.

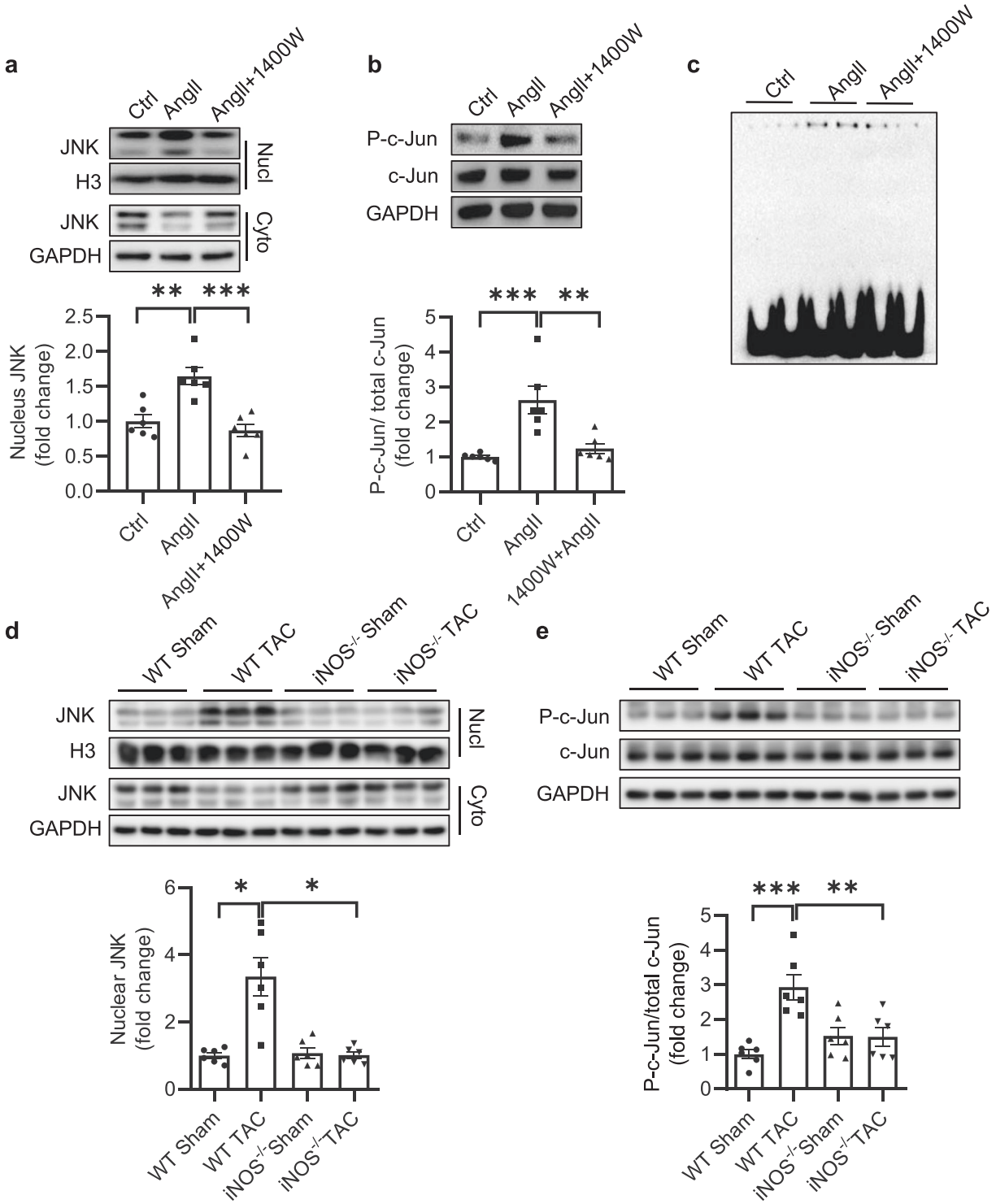

Fig. 6 Inhibition of SNO-JNK improves cardiac fibrosis through deactivating c-Jun/AP-1 pathway in vitro and vivo. NRCFs were pre-incubated with 1400 W for 1 h followed by treatment with Ang II (100 nM) or control PBS. **a** Cytoplasmic and nuclear proteins were separately extracted and analyzed by SDS-PAGE to determine the level of nuclear JNK. $n = 6$ for each group. **b** Total protein was extracted and analyzed by SDS-PAGE to determine the phosphorylation of c-Jun (P-c-Jun). $n = 6$ for each group. **c** EMSA was used to determine the binding activity of AP-1 to its reactive elements. Eight-week-old of C57BL/6 and iNOS-knockout mice were subjected to TAC for four weeks. **d** Heart tissues in each group were collected, cytoplasmic and nuclear proteins were extracted and analyzed by SDS-PAGE to determine the level of nuclear JNK. $n = 6$ for each group. **e** Total protein was extracted and analyzed by SDS-PAGE to determine the phosphorylation of c-Jun (P-c-Jun). $n = 6$ for each group. The results are represented as the mean ± SEM. (*$P < 0.05$, **$P < 0.01$, and ***$P < 0.001$). **a**, **b**, and **e**. One-way ANOVA was used for statistical analysis; **d** Kruskal–Wallis test was used for statistical analysis.

Similarly, the binding activity of AP-1, a downstream effector of c-Jun/AP-1 signaling pathway, was notably reduced with 1400 W pretreatment as determined by EMSA (Fig. 6c). We then isolated the nuclear and cytoplasmic components of heart tissues in iNOS$^{-/-}$ and WT littermates subjected to TAC, and detected the levels of JNK. In accordance with the in vitro observations, nuclear levels of JNK robustly increased in the hearts of WT mice subjected to TAC, while this increase was not observed in iNOS$^{-/-}$ mice (Fig. 6d). Finally, the increased phosphorylation of c-Jun observed in the hearts of WT TAC mice was reduced in the iNOS$^{-/-}$ TAC mice (Fig. 6e). These in vivo results confirm the previous in vitro observations that iNOS-induced S-nitrosylation of JNK induces cardiac fibrosis through activating c-Jun/AP-1 pathway.

DISCUSSION

We presented a novel mechanism underlying JNK activation during cardiac fibrosis. An increase in SNO-JNK in the context of cardiac fibrosis was observed in both rodent and human heart tissue. S-Nitrosylation of JNK at Cys116 and Cys163 accelerates cardiac fibrosis by activating c-Jun phosphorylation and the subsequent transcriptional activity of AP-1, leading to increased expression of pro-fibrotic genes.

JNK plays a pivotal role in the convergence of multiple signalling pathways in pathophysiological processes, including various cardiac diseases. For instance, in cardiac ischaemia/reperfusion (IR) injury, activation of JNK aggravates mitochondrial metabolism disorder by inducing mitochondrial fission/mitophagy [29]. In diabetic cardiomyopathy, high glucose (HG)-induced phosphorylation of JNK is the upstream regulator of NF-κB-mediated myocardial inflammation and apoptosis [30]. In the current study, we used a pressure overload-induced interstitial fibrosis model and found an elevation of SNO-JNK, indicating the involvement of SNO-JNK during cardiac fibrosis. To confirm the specific role of SNO-JNK in cardiac fibrosis, NRCFs were transfected with JNK-C116A/163A cells resistant to S-nitrosylation. The JNK-C116A/163A mutant alleviated the pro-fibrotic effects of AngII in NRCFs. Moreover, 1400 W, an inhibitor of iNOS that promoted SNO-JNK, was proven to reduce AngII-induced cardiac fibroblast differentiation in NRCFs. Finally, iNOS knockout substantially reduced SNO-JNK and alleviated cardiac interstitial fibrosis in TAC mice, further confirming the specific role of SNO-JNK in cardiac fibrosis.

It should be noted that the observed loss-of-function by the C116/C163A mutation is derived from the failure to the SNO modify rather than directly disrupting the JNK molecular structure for its kinase activity. Previous work by Nelson and coauthors constructed multiple JNK expression vectors with mutations from cysteine to alanine, including C116A and C163A, and found that these mutations did not affect the protein level or kinase activity of JNK [31]. Similar results were observed in another study in which JNK mutations from cysteine to serine (C116S) maintained kinase activity [24, 32]. Although Hee-Sae Park and coworkers found that S-nitrosylation of JNK at Cys116 plays an important role in INF-γ-treated macrophages, we found another new S-nitrosylation site of JNK in cardiac fibrosis [24]. In addition, previous work found that S-nitrosylation of JNK at Cys116 represses the interaction between JNK and c-jun, thus inhibiting the phosphorylation and transactivation of c-jun; however, we observed the opposite process [24]. These results demonstrate the complicated biological function of SNO-JNK in different conditions, whose downstream effectors can be either positively or negatively regulated. There are also similar observations that iNOS-dependent S-nitrosylation of JNK3 (a JNK isoform selectively expressed in the brain and heart) increases phosphorylation of JNK3 and exacerbates global ischaemia/reperfusion injury in the rat hippocampus [33]. Although different cell microenvironments might cause this inconsistency, the specific mechanism of discrepant responses to S-nitrosylation in different conditions remains to be identified. In addition, how S-nitrosylation of JNK affects JNK activity remains an open question. Since S-nitrosylation can influence the protein–protein interactions, we proposed that S-nitrosylation of JNK might affect the interaction of JNK with other kinases or phosphatases, which requires further investigation.

Gaseous signalling molecules, including nitric oxide (NO) and hydrogen sulfide (H_2S) are important in cellular processes associated with the cardiovascular system [34–38]. Gaseous signalling molecule-mediated post-translational modifications of cysteine modulate various cardiovascular diseases. Previously, we found that S-sulfhydration of cysteine was important for endothalial and cardiomyocyte homeostasis [19, 27, 39–41]. Accordingly, restoration of cysteine balance has therapeutic benefits. It is widely accepted that protein S-nitrosylation is regulated intricately. The spatial and temporal regulation of S-nitrosylation/de-nitrosylation of functional proteins confers the specific effects of NO both in physiological and pathological conditions. For example, S-nitrosylation of β-arrestin biases G protein-coupled receptor(GPCRs) signalling by suppressing canonical β-arrestin function and supports adrenergic function in failing hearts [42]. iNOS induces activation of cyclooxygenase-2 (COX2) through binding and promoting S-nitrosylation of COX2 during inflammation. Sustained activation of iNOS is considered the main endogenous source of S-nitrosylation in the cardiovascular system. In this way, iNOS agonists have been developed as potential therapeutic agents for the treatment of ischaemia/reperfusion injury (IR), type II diabetes mellitus (T2DM) and heart failure (HF) [43]. On the other hand, de-nitrosylation can be induced by thioredoxin (TRX), an oxidoreductase and S-nitrosoglutathione reductase (GSNOR) [44]. In microvascular endothelial cells, the expression of iNOS requires redox regulation [45], while iNOS deficiency in smooth muscle cells in turn alters the AP1/Ref-1 redox pathway [46]. Therefore, it is rational to propose that S-nitrosylation can transduce cellular redox status to kinase signalling, which influences a variety of cellular functions.

In conclusion, this study shows that iNOS-induced S-nitrosylation of JNK at Cys116 and Cys163 accelerates cardiac fibrosis, via c-Jun phosphorylation and AP-1 activation, resulting in the increased expression of pro-fibrotic genes. These data uncover a new fundamental molecular mechanism underlying cardiac fibrosis via the iNOS/SNO-JNK/AP-1 pathway, and provide a novel therapeutic strategy for heart diseases.

ACKNOWLEDGEMENTS

The authors are grateful to Dr Qiu-lun Lu for proofing the article. This work was supported by grants from the National Key Research and Development Program of China (2019YFA0802704). National Natural Science Foundation of China (grant NOs. 82030013, 81820108002, 81800213, 81870183). Natural Science Foundation of Jiangsu Province (BK20180680). Natural Science Foundation of Jiangsu Higher Education Institutions of China (19KJA360004).

AUTHOR CONTRIBUTIONS

YJ, SSL designed the research; SSL wrote the paper; JYC, MZ, MLC performed the in vitro experiments; MZ, XCZ, CZ performed in vivo research; MZ, MLC, ZGS, XCZ, LPX analyzed data; SXS helped to perform the in vivo experiments, ZRH helped to collect the clinical samples.

ADDITIONAL INFORMATION

Supplementary information The online version contains supplementary material available at https://doi.org/10.1038/s41401-021-00674-9.

Competing interests: The authors declare no competing interests.

REFERENCES

1. Gabbiani G. The myofibroblast in wound healing and fibrocontractive diseases. J Pathol. 2003;200:500–3.
2. Lopez B, Gonzalez A, Ravassa S, Beaumont J, Moreno MU, San Jose G, et al. Circulating biomarkers of myocardial fibrosis: the need for a reappraisal. J Am Coll Cardiol. 2015;65:2449–56.
3. Cokkinos DV, Pantos C. Myocardial remodeling, an overview. Heart Fail Rev. 2011;16:1–4.
4. Meng G, Xiao Y, Ma Y, Tang X, Xie L, Liu J, et al. Hydrogen sulfide regulates kruppel-like factor 5 transcription activity via specificity protein 1 S-sulfhydration at Cys664 to prevent myocardial hypertrophy. J Am Heart Assoc. 2016;5:1–17.
5. Meng G, Liu J, Liu S, Song Q, Liu L, Xie L, et al. Hydrogen sulfide pretreatment improves mitochondrial function in myocardial hypertrophy via a SIRT3-dependent manner. Br J Pharmacol. 2018;175:1126–45.
6. Yu SS, Cai Y, Ye JT, Pi RB, Chen SR, Liu PQ, et al. Sirtuin 6 protects cardiomyocytes from hypertrophy in vitro via inhibition of NF-kappaB-dependent transcriptional activity. Br J Pharmacol. 2013;168:117–28.
7. He X, Gao X, Peng L, Wang S, Zhu Y, Ma H, et al. Atrial fibrillation induces myocardial fibrosis through angiotensin II type 1 receptor-specific Arkadia-mediated downregulation of Smad7. Circ Res. 2011;108:164–75.
8. McCarthy CA, Widdop RE, Denton KM, Jones ES. Update on the angiotensin AT_2 receptor. Curr Hypertens Rep. 2013;15:25–30.
9. Lin Z, Altaf N, Li C, Chen M, Pan L, Wang D, et al. Hydrogen sulfide attenuates oxidative stress-induced NLRP3 inflammasome activation via S-sulfhydrating c-Jun at Cys269 in macrophages. Biochim Biophys Acta Mol Basis Dis. 2018;1864:2890–900.
10. Lu G, Xu S, Peng L, Huang Z, Wang Y, Gao X. Angiotensin II upregulates Kv1.5 expression through ROS-dependent transforming growth factor-beta1 and extracellular signal-regulated kinase 1/2 signalings in neonatal rat atrial myocytes. Biochem Biophys Res Commun. 2014;454:410–6.
11. Liu W, Ruiz-Velasco A, Wang S, Khan S, Zi M, Jungmann A, et al. Metabolic stress-induced cardiomyopathy is caused by mitochondrial dysfunction due to attenuated Erk5 signaling. Nat Commun. 2017;8:494.
12. Yan J, Kong W, Zhang Q, Beyer EC, Walcott G, Fast VG, et al. c-Jun N-terminal kinase activation contributes to reduced connexin43 and development of atrial arrhythmias. Cardiovasc Res. 2013;97:589–97.
13. Zhu J, Zhang J, Huang H, Li J, Yu Y, Jin H, et al. Crucial role of c-Jun phosphorylation at Ser63/73 mediated by PHLPP protein degradation in the cheliensisin a inhibition of cell transformation. Cancer Prev Res (Philos). 2014;7:1270–81.
14. Sha Y, Marshall HE. S-nitrosylation in the regulation of gene transcription. Biochim Biophys Acta. 2012;1820:701–11.
15. Shvedova M, Anfinogenova Y, Atochina-Vasserman EN, Schepetkin IA, Atochin DN. c-Jun N-Terminal Kinases (JNKs) in myocardial and cerebral ischemia/reperfusion injury. Front Pharmacol. 2018;9:715.
16. Manoury B, Montiel V, Balligand JL. Nitric oxide synthase in post-ischaemic remodelling: new pathways and mechanisms. Cardiovasc Res. 2012;94:304–15.
17. Stomberski CT, Hess DT, Stamler JS. Protein S-Nitrosylation: determinants of specificity and enzymatic regulation of S-Nitrosothiol-Based Signaling. Antioxid Redox Signal. 2019;30:1331.
18. Sun J, Murphy E. Protein S-nitrosylation and cardioprotection. Circ Res. 2010;106:285–96.
19. Wang W, Wang D, Kong C, Li S, Xie L, Lin Z, et al. eNOS S-nitrosylation mediated OxLDL-induced endothelial dysfunction via increasing the interaction of eNOS with betacatenin. Biochim Biophys Acta Mol Basis Dis. 2019;1865:1793–801.
20. Mattera R, Benvenuto M, Giganti MG, Tresoldi I, Pluchinotta FR, Bergante S, et al. Effects of polyphenols on oxidative stress-mediated injury in cardiomyocytes. Nutrients. 2017;9:1–43.
21. Crowley SD. The cooperative roles of inflammation and oxidative stress in the pathogenesis of hypertension. Antioxid Redox Signal. 2014;20:102–20.
22. Ishihara Y, Takemoto T, Itoh K, Ishida A, Yamazaki T. Dual role of superoxide dismutase 2 induced in activated microglia: oxidative stress tolerance and convergence of inflammatory responses. J Biol Chem. 2015;290:22805–17.
23. Holmes S, Singh M, Su C, Cunningham RL. Effects of oxidative stress and testosterone on pro-inflammatory signaling in a female rat dopaminergic neuronal cell line. Endocrinology 2016;157:2824–35.
24. Park HS, Huh SH, Kim MS, Lee SH, Choi EJ. Nitric oxide negatively regulates c-Jun N-terminal kinase/stress-activated protein kinase by means of S-nitrosylation. Proc Natl Acad Sci USA. 2000;97:14382–7.
25. Stamler JS, Simon DI, Jaraki O, Osborne JA, Francis S, Mullins M, et al. S-nitrosylation of tissue-type plasminogen activator confers vasodilatory and antiplatelet properties on the enzyme. Proc Natl Acad Sci USA. 1992;89:8087–91.
26. Pan L, Lin Z, Tang X, Tian J, Zheng Q, Jing J, et al. S-Nitrosylation of Plastin-3 exacerbates thoracic aortic dissection formation via endothelial barrier dysfunction. Arterioscler Thromb Vasc Biol. 2020;40:175–88.
27. Tang X, Pan L, Zhao S, Dai F, Chao M, Jiang H, et al. SNO-MLP (S-Nitrosylation of Muscle LIM Protein) facilitates myocardial hypertrophy through TLR3 (Toll-Like Receptor 3)-mediated RIP3 (receptor-interacting protein kinase 3) and NLRP3 (NOD-Like receptor pyrin domain containing 3) inflammasome activation. Circulation. 2020;141:984–1000.
28. Kong M, Chen X, Lv F, Ren H, Fan Z, Qin H, et al. Serum response factor (SRF) promotes ROS generation and hepatic stellate cell activation by epigenetically stimulating NCF1/2 transcription. Redox Biol. 2019;26:101302.
29. Jin Q, Li R, Hu N, Xin T, Zhu P, Hu S, et al. DUSP1 alleviates cardiac ischemia/reperfusion injury by suppressing the Mff-required mitochondrial fission and Bnip3-related mitophagy via the JNK pathways. Redox Biol. 2018;14:576–87.
30. Pan Y, Wang Y, Zhao Y, Peng K, Li W, Wang Y, et al. Inhibition of JNK phosphorylation by a novel curcumin analog prevents high glucose-induced inflammation and apoptosis in cardiomyocytes and the development of diabetic cardiomyopathy. Diabetes. 2014;63:3497–511.
31. Nelson KJ, Bolduc JA, Wu H, Collins JA, Burke EA, Reisz JA, et al. H_2O_2 oxidation of cysteine residues in c-Jun N-terminal kinase 2 (JNK2) contributes to redox regulation in human articular chondrocytes. J Biol Chem. 2018;293:16376–89.
32. Park HS, Park E, Kim MS, Ahn K, Kim IY, Choi EJ. Selenite inhibits the c-Jun N-terminal kinase/stress-activated protein kinase (JNK/SAPK) through a thiol redox mechanism. J Biol Chem. 2000;275:2527–31.
33. Yu HM, Xu J, Li C, Zhou C, Zhang F, Han D, et al. Coupling between neuronal nitric oxide synthase and glutamate receptor 6-mediated c-Jun N-terminal kinase signaling pathway via S-nitrosylation contributes to ischemia neuronal death. Neuroscience. 2008;155:1120–32.
34. Meng G, Zhu J, Xiao Y, Huang Z, Zhang Y, Tang X, et al. Hydrogen sulfide donor GYY4137 protects against myocardial fibrosis. Oxid Med Cell Longev. 2015;2015:691070.
35. Meng G, Ma Y, Xie L, Ferro A, Ji Y. Emerging role of hydrogen sulfide in hypertension and related cardiovascular diseases. Br J Pharmacol. 2015;172:5501–11.
36. Xie L, Feng H, Li S, Meng G, Liu S, Tang X, et al. SIRT3 Mediates the antioxidant effect of hydrogen sulfide in endothelial cells. Antioxid Redox Signal. 2016;24:329–43.
37. Meng G, Wang J, Xiao Y, Bai W, Xie L, Shan L, et al. GYY4137 protects against myocardial ischemia and reperfusion injury by attenuating oxidative stress and apoptosis in rats. J Biomed Res. 2015;29:203–13.
38. Liu Z, Han Y, Li L, Lu H, Meng G, Li X, et al. The hydrogen sulfide donor, GYY4137, exhibits anti-atherosclerotic activity in high fat fed apolipoprotein $E^{(-/-)}$ mice. Br J Pharmacol. 2013;169:1795–809.
39. Zheng Q, Pan L, Ji YH. 2S protects against diabetes-accelerated atherosclerosis by preventing the activation of NLRP3 inflammasome. J Biomed Res. 2019;34:94–102.
40. Meng G, Zhao S, Xie L, Han Y, Ji Y. Protein S-sulfhydration by hydrogen sulfide in cardiovascular system. Br J Pharmacol. 2018;175:1146–56.
41. Xie L, Gu Y, Wen M, Zhao S, Wang W, Ma Y, et al. Hydrogen sulfide induces Keap1 S-sulfhydration and suppresses diabetes-accelerated atherosclerosis via Nrf2 activation. Diabetes. 2016;65:3171–84.
42. Irie T, Sips PY, Kai S, Kida K, Ikeda K, Hirai S, et al. S-Nitrosylation of calcium-handling proteins in cardiac adrenergic signaling and hypertrophy. Circ Res. 2015;117:793–803.
43. Soskic SS, Dobutovic BD, Sudar EM, Obradovic MM, Nikolic DM, Djordjevic JD, et al. Regulation of inducible nitric oxide synthase (iNOS) and its potential role in insulin resistance. Diabetes Heart Fail Open Cardiovasc Med J. 2011;5:153–63.
44. Benhar M, Forrester MT, Stamler JS. Protein denitrosylation: enzymatic mechanisms and cellular functions. Nat Rev Mol Cell Biol. 2009;10:721–32.
45. Wu F, Tyml K, Wilson JX. iNOS expression requires NADPH oxidase-dependent redox signaling in microvascular endothelial cells. J Cell Physiol. 2008;217:207–14.
46. Chyu KY, Dimayuga PC, Zhao X, Nilsson J, Shah PK, Cercek B. Altered AP-1/Ref-1 redox pathway and reduced proliferative response in iNOS-deficient vascular smooth muscle cells. Vasc Med. 2004;9:177–83.